Biophysical Chemistry 308 (2024) 107217

Contents lists available at ScienceDirect

Biophysical Chemistry

journal homepage: www.elsevier.com/locate/biophyschem

H_2 production under stress: [FeFe]-hydrogenases reveal strong stability in high pressure environments

Kristina Edenharter [a], Michel W. Jaworek [b], Vera Engelbrecht [a], Roland Winter [b,*], Thomas Happe [a,*]

[a] Photobiotechnology, Faculty of Biology and Biotechnology, Ruhr-University Bochum, 44801 Bochum, Germany
[b] Physical Chemistry I - Biophysical Chemistry, Department of Chemistry and Chemical Biology, TU Dortmund University, Otto-Hahn-Straße 4a, 44227 Dortmund, Germany

ARTICLE INFO

Keywords:
Enzymatic reactions
High pressure
Hydrogenases

ABSTRACT

Hydrogenases are a diverse group of metalloenzymes that catalyze the conversion of H_2 into protons and electrons and the reverse reaction. A subgroup is formed by the [FeFe]-hydrogenases, which are the most efficient enzymes of microbes for catalytic H_2 conversion. We have determined the stability and activity of two [FeFe]-hydrogenases under high temperature and pressure conditions employing FTIR spectroscopy and the high-pressure stopped-flow methodology in combination with fast UV/Vis detection. Our data show high temperature stability and an increase in activity up to the unfolding temperatures of the enzymes. Remarkably, both enzymes reveal a very high pressure stability of their structure, even up to pressures of several kbars. Their high pressure-stability enables high enzymatic activity up to 2 kbar, which largely exceeds the pressure limit encountered by organisms in the deep sea and sub-seafloor on Earth.

1. Introduction

[FeFe]-hydrogenases are fascinating enzymes that play an important role in the reversible conversion of molecular hydrogen (H_2) into protons and electrons, making them essential players in microbial H_2 metabolism. The use of readily available earth-abundant metals and their impressive turnover rates, reaching up to 10,000 molecules per second, make these enzymes perfect candidates for the production of sustainable H_2 [1,2]. [FeFe]-hydrogenases are found in fermentative anaerobic organisms and some eukaryotes (e.g., green algae), where they are part of the H_2 metabolism [3]. The catalytic center of [FeFe]-hydrogenases, called the H-cluster, is composed of a cubane [4Fe—4S] subcluster and a unique [2Fe—2S] cluster, which are coupled through a coordinating cysteine residue. The two Fe atoms of the [2Fe—2S] cluster, termed proximal iron (Fe_p) and distal iron (Fe_d) according to their location to the [4Fe—4S] cluster, are coordinated by an azadithiolate (adt) ligand, three carbon monoxide (CO) and two cyanide (CN^-) ligands. [4–7] The Fe_d has already been identified as the actual site of catalysis [8–10]. The H-cluster is part of a highly conserved domain (H-domain) formed by two four-stranded β-sheets and several α-helices. This M1-subtype is the simplest form and has only been found in Chlorophycean green algae [9,11,12]. In addition to the H-domain, further iron-sulfur (Fe—S) cluster-containing domains can occur, which serve as electron relays and transport electrons from the electron donor to the H-cluster, the site of catalysis (M2-, M3-subtype) [13,14]. A representative of the M2-subtype is the homodimeric [FeFe]hydrogenase $CbA5H_{WT}$ from *Clostridium beijerinckii*, which has been studied extensively in recent years due to its oxygen (O_2) stability [15,16]. $CbA5H_{WT}$ is mainly characterized by the fact that the O_2-protected state (H_{inact}) is reversible, i.e., after removal of O_2, $CbA5H_{WT}$ can be reactivated (H_{ox}). This process can be repeated several times without significant loss of activity [14,15]. Responsible for this O_2 tolerance is a conserved cysteine residue C367 in the immediate vicinity of the H-cluster, which approaches the Fe_d under oxidative conditions by structural rearrangement of the hydrogenase and thus prevents the binding of O_2 to the H-cluster. Furthermore, it was shown that the flip of the cysteine residue could only be made possible by the increased flexibility of the so-called TSC peptide loop compared to other standard hydrogenases, such as CpI_{WT} from *Clostridium pasteurianum* [16].

M3-subtype [FeFe]-hydrogenases, such as CpI_{WT}, are probably the most common form of [FeFe]-hydrogenases in Clostridia. [17,18] When comparing CpI_{WT} and $CbA5H_{WT}$ on a structural level, it has already been

* Corresponding authors.
E-mail addresses: roland.winter@tu-dortmund.de (R. Winter), thomas.happe@ruhr-uni-bochum.de (T. Happe).

https://doi.org/10.1016/j.bpc.2024.107217
Received 22 February 2024; Accepted 10 March 2024
Available online 11 March 2024

shown that in the case of CpI_{WT}, the interaction of different residues ensures that the cysteine residue C299 cannot protect the active site Fe_d from damage under aerobic conditions. An exchange of the corresponding amino acid positions of CpI_{WT} in $CbA5H_{WT}$ ensured that the conformational change occurred more slowly and an increased O_2 sensitivity of the variants compared to the WT was observed [16].

As the field of high-pressure enzymology continues to evolve, the study of the effects of high pressure on [FeFe]-hydrogenases has become a fascinating area of research, providing crucial insights into their structure, stability and function under extreme environmental conditions. High hydrostatic pressure (HHP) effects on enzyme activity and stability have already provided valuable insights into the behavior of enzymes towards extreme conditions [19–28]. These studies showed that high pressure can lead to conformational changes, alter protein dynamics and significantly affect the stability and catalytic properties of enzymes. Catalytic activity can be directly enhanced by HHP if the activation volume associated with the reaction is negative, and HHP can alter the substrate specificity and stereoselectivity of an enzyme [25,26]. Further, given that the rate of an enzymatic reaction is often limited by the thermostability of the enzyme, superimposing pressure-induced thermostabilization of the enzyme with an accelerated substrate conversion at increased temperatures can lead to improved overall reaction rates. This holds true for proteins exhibiting elliptic-like phase diagrams in the *p*, *T*-plane [25–27]. A study on α-chymotrypsin showed an increased catalytic activity and stability against thermal denaturation. At 20 °C and an applied pressure of 4.7 kbar, the catalytic activity increased by a factor of 6.5 compared to measurements under atmospheric pressure. The accelerating effect at a pressure of 1.8 kbar at 55 °C was shown to be almost 20 times higher than at 1 bar and the same temperature [27]. The activity of designed catalytic amyloid fibrils revealed not only a remarkably high pressure and temperature stability of the systems, but also enhanced esterase activity at high pressure as a consequence of a negative activation volume at all temperatures [22]. Gerringer et al. examined the muscle tissue of various fish species living at different ocean depths to investigate lactate dehydrogenase (LDH) and malate dehydrogenase (MDH) [28]. The deep-sea fish exhibited an elevation in LDH activity in response to pressure, while the enzymes in shallow-water species displayed a decrease in activity [29]. Whereas monomeric proteins are generally rather pressure stable up to 4–8 kbar, oligomeric proteins are often prone to pressure-induced dissociation of the protein complex in the kbar pressure regime [25,26]. Markandeswar and Horowitz showed dissociation of single ring heptameric GroEL chaperone by hydrostatic pressures up to 3 kbar [30].

Despite their enormous importance, the stability and activity of [FeFe]-hydrogenases from mesophilic organisms at extreme temperature and pressure conditions are still largely *terra incognita*. In this study, we investigated the influence of temperature and pressure on two wild-type [FeFe]-hydrogenases, $CbA5H_{WT}$ and CpI_{WT} (Fig. 1), focusing in particular on their structural and functional responses to elevated pressures up to the kbar regime. For this purpose, Fourier-transform infrared (FTIR) spectroscopy and the high-pressure stopped-flow (HPSF) methodology in combination with fast UV/Vis spectroscopy were employed. To follow the hydrogenase reaction, the formation of H_2 was measured in a direct and an indirect way using methyl viologen.

2. Experimental section

2.1. Protein expression and isolation

The pET21b vector containing either the $CbA5H_{WT}$ gene codon-optimized for *E. coli* (NCBI GenBank: KX147468.1) or the CPI_{WT} gene (GenBank: M81737.1) served as the expression plasmid. Heterologous expression of the apo-hydrogenases was performed under anaerobic conditions in an anoxic tent under a N_2/H_2 atmosphere (99:1) as previously described [31]. For isolation of the proteins, 2 mM sodium dithionite (NaDT) was added to all buffers used. Protein purification was performed by affinity chromatography by C-terminal StrepII tag. Protein solutions were concentrated using Amicon Ultra centrifugal filter (30 kDa) and stored in 0.1 M Tris-HCl (Tris(hydroxymethyl)-aminomethane), pH 8.0, supplemented with 2 mM NaDT at −80 °C. Concentration determination according to Bradford was followed by determination of the purity and molecular weight of the protein solution by polyacrylamide gel electrophoresis (SDS-PAGE) [32].

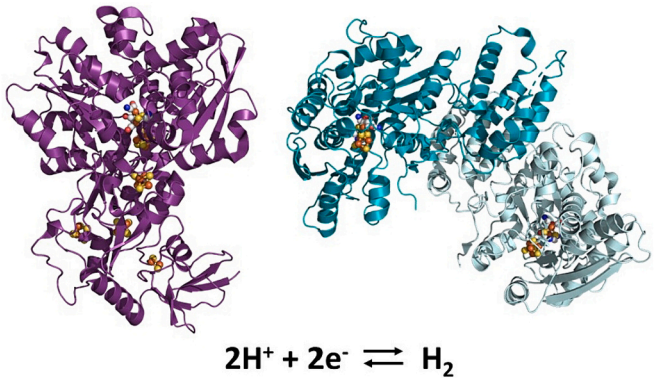

Fig. 1. Cartoon structure of CpI_{WT} (PDB ID: 4XDC; purple) and $CbA5H_{WT}$ (PDB ID: 6TTL; chain A presented in teal and chain B presented in light blue) and the H_2-production reaction. The H-Cluster and accessory FeS clusters are depicted as ball-stick model. (For interpretation of the references to colour in this figure legend, the reader is referred to the web version of this article.)

2.2. In vitro maturation

To complete the active site of the hydrogenases, in vitro maturation was performed [5]. For this purpose, the purified apo-protein, which possessed only the [4Fe—4S] cluster, was incubated with a 5× molar excess of adt cofactor in 0.1 M KPI (potassium phosphate buffer), pH 6.8, for 1 h on ice. Size exclusion was used to separate the holo-protein from the unbound adt cofactor.

2.3. Temperature dependent H_2-production assay

To determine the H_2 production activity of the hydrogenases in a temperature-dependent manner, 400 ng of holo-hydrogenase was incubated in 2 mL test mixtures consisting of 100 mM NaDT, 10 mM MV (methyl viologen) and KPI buffer, pH 6.8, in 8 mL vessels (Suba). After purging the sample with 100% argon for 5 min, the test mixtures were incubated for 20 min at 25–75 °C at 100 rpm in a shaking water bath. Subsequently, H_2 production could be verified by analyzing 400 μL of the gas phase by gas chromatography (Shimadzu).

2.4. Fourier-transform infrared (FTIR) spectroscopy measurements

Before investigating the structural stability of the hydrogenases as a function of temperature and pressure, an H/D exchange was carried out on the respective apo-protein. To this end, the hydrogenase was dialyzed against D_2O using Amicon Ultra centrifugation units with 30 kDa cutoff, and subsequently lyophilized and purified by dialysis to remove the additives, respective water molecules. The pD (pH +0.4 = pD) for each solution was adjusted to 8 by adding DCl to the Tris (D_2O) buffer solution. The final protein concentration amounted 5 wt%.

Temperature- and pressure-dependent FTIR measurements were performed using a Nicolet 6700 (Thermo Fisher Scientific) spectrometer equipped with a liquid-nitrogen cooled MCT-detector (HgCdTe). 20 μL of the sample was placed between two CaF_2 windows separated by a mylar spacer, which was integrated in the temperature cell. An external circulating water thermostat with a digital thermometer placed in the sample controlled the required temperature. The temperature was

equilibrated for ~10 min before spectra were collected. 128 scans per measurement (3 min) were recorded and averaged in the wavenumber range between 4000 and 650 cm^{-1} with a spectral resolution of 2 cm^{-1}. High pressures up to 10 kbar could be achieved using a membrane-driven diamond anvil cell (Diacells VivoDac, Almax easyLab), equipped with type IIa diamonds (Almax easyLab), which were connected to an automated pneumatic pressure controller (Diacells iGM Controller, Almax easyLab). Here, a 50 μm thick brass gasket was placed between the two diamond windows, holding 3 μL of the sample (effective sample volume ~ 10 nL). The stretching vibration of SO_4^{2-} in crystalline $BaSO_4$ was used as an internal pressure calibrant [33].

Data analysis was carried out using the Thermo Grams 8.0 software. After buffer subtraction and smoothing of each spectrum, the area of the amide I′ band (1700–1600 cm^{-1}) was normalized to 1. The numbers and positions of the subbands could be determined by using two mathematical operations, Fourier self-deconvolution (FSD) and 2nd derivative analysis, to identify the position of the secondary structure elements and to evaluate conformational changes [34]. In addition, the secondary structure components from the pdb database ($CbA5H_{WT}$: 6TTL & CpI_{WT}: 6GM2) were used for assistance. The amide I′ band region of the proteins could be decomposed into six subbands, and mixed Gaussian–Lorentzian line shape functions were used to the fit the peak areas and to determine the relative changes in the population of secondary structure elements [35].

Assuming a two-state unfolding process for the hydrogenases, the sigmoidal curve progression of the secondary structure elements could be fitted by using the Boltzmann function. In the case of temperature-induced unfolding, the infrared absorbance intensity is given by

$$I = \frac{I_f - I_u}{1 + e^{-(T-T_u)\bullet\left(\Delta H^{\circ}_{vH}/R\right)}} + I_u \quad (1)$$

where I_f and I_u are the plateau intensity values for the folded and unfolded state of the protein, respectively, and T_u describes the unfolding temperature at the midpoint of the transition. The standard van't Hoff enthalpy change, ΔH°_{vH}, can be directly obtained from the slope of the curves. All measurements were done at least in triplicate.

2.5. High-pressure stopped-flow measurements of enzymatic activity

A high-pressure stopped-flow (HPSF) instrument (HPSF-56) was used to measure the enzyme activity at different pressures [36]. The pressures assayed were 1, 1000 and 2000 bar. Both the substrate solution, containing 160 μM methyl viologen and NaDT each in 0.1 M Tris-HCl pH 8.0 buffer, and the protein solution (0.6 μM of the protein of interest in 0.1 M Tris-HCl, pH 8.0 buffer) were prepared under strict anaerobic conditions and sealed airtight in 20 mL vessels. Before injection of the solutions into the measuring cell, the sample cell as well as the chamber were purged with nitrogen and the cell immediately sealed with sticky tape. To inject the substrate or protein solution, syringes were first rinsed with 0.1 M Tris-HCl, pH 8.0, containing 2 mM NaDT to prevent contamination with O_2. Subsequently, syringes were rinsed again with 0.1 M Tris-HCl pH 8.0 buffer to remove NaDT from the syringe. The enzyme concentration was maintained at 0.3 μM post-mixing for all activity assays with post-mixing substrate concentrations of 80 μM. The initial velocity of the enzyme reaction, v_0, was monitored for 1.5–15 s post-mixing and was determined by calculating $v_0 = d[P]/dt$, where [P] represents the formation of the oxidized methyl viologen, from the slope of the linear fit of the time dependent absorbance data at 604 nm, which has a molar extinction coefficient of 13.600 M^{-1} cm^{-1} [37]. Temperature was controlled and maintained at 25 °C by a thermostat.

3. Results and discussion

3.1. Temperature dependent H_2-production activity assay

To investigate the influence of temperature on the H_2 production activity of the tested proteins, the in vitro test mixtures were incubated at different temperatures before the H_2 content in the gas phase was measured by gas chromatography. The measurements show that both enzymes have similar activity profiles with an optimum between 45 and 65 °C (Fig. 2). However, it is noticeable that the temperature optimum of CpI_{WT} is slightly lower (45–55 °C) in contrast to $CbA5H_{WT}$ (55–65 °C). As expected, the enzymatic activity increases with increasing temperature, by a factor 2–3 over a temperature range of 30 °C. The comparison with the unfolding temperatures, T_u, of the different enzymes (see below) reveals that the maximum activity is limited by the temperature-induced unfolding of the enzymes.

3.2. Temperature and pressure dependent analysis of the secondary structure

To explore the temperature- and pressure-induced conformational changes of the hydrogenases, FTIR spectroscopy measurements were employed in Tris (D_2O) buffer. The amide-I′ band region was analyzed by using a fitting procedure that yields quantitative information about the respective fractions of secondary structure elements of the proteins. The normalized amide I′ band of $CbA5H_{WT}$ as a function of temperature (Fig. 3A) shows a broad band at ~1650 cm^{-1}, which decreases slightly with increasing temperature. Above a certain temperature, two peaks appear, at ~1617 cm^{-1} and ~1683 cm^{-1}, respectively, indicating unfolding and subsequent aggregation of the protein forming intermolecular β-sheets. The secondary structure elements determined are in good agreement with crystallographic data obtained by Winkler et al., which show a dominance of the fraction of α-helices [16]. Small percentage differences in α-helix and intramolecular β-sheet contents are supposed to be due to different absorption coefficients of the secondary

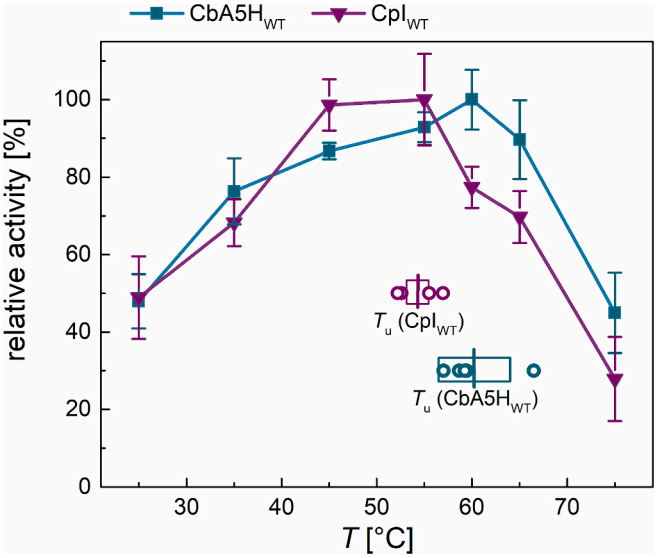

Fig. 2. Temperature dependent H_2 production activity of $CbA5H_{WT}$ and CpI_{WT}. The H_2 production activity was determined for different temperatures between 25 and 75 °C. Relative values correlate with the percentage of maximum activity ($CbA5H_{WT}$: 2794.94 ± 216.49 μM H_2 mg^{-1} [E] min^{-1}; CpI_{WT}: 3027.04 ± 357.42 μM H_2 mg^{-1} [E] min^{-1} achieved across the entire temperature range). All data points are mean values ± standard deviation from two biological replicates and three technical replicates for each measurement. Additionally, spectroscopically determined unfolding temperatures, T_u, were inserted in boxes, where the widths of the box indicate the error bar in determining T_u.

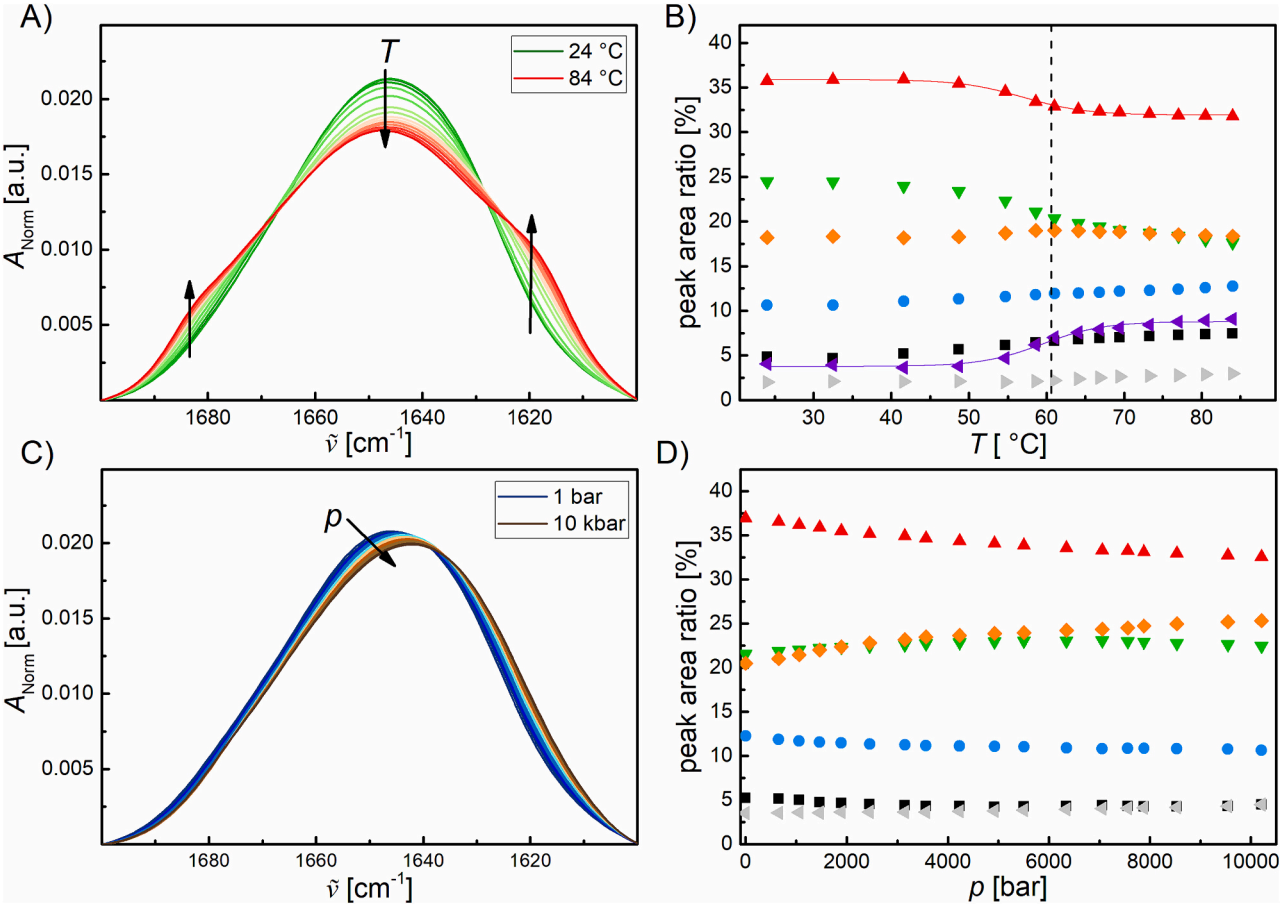

Fig. 3. Temperature- and pressure-dependent FTIR absorption data of $CbA5H_{WT}$ in Tris (D_2O) buffer (A–D). Left: Normalized amide I′ band, right: respective secondary structure elements of temperature- and pressure-induced changes. The temperature-dependent measurements were recorded at ambient pressure (1 bar), the pressure dependent measurements at $T = 25$ °C. β-sheets (1680 cm^{-1}, black), turns and loops (1672 cm^{-1}, blue), α-helices (1654 cm^{-1}, red), random coils (1642 cm^{-1}, green), intramolecular β-sheets (1636 cm^{-1}, orange), intermolecular β-sheets (1617 cm^{-1}, purple), and side chains (1610 cm^{-1}, gray). Lines display the Boltzmann fits to the experimental data using eq. (1) and the dashed line represents the midpoint of T_u. (For interpretation of the references to colour in this figure legend, the reader is referred to the web version of this article.)

structure elements. Beyond a temperature of ~50 °C, temperature-induced unfolding and denaturation sets in, which can be seen in a decrease of the amount of α-helices (~ −3%) and unordered structures (~ −7%), with concomitant formation of antiparallel intermolecular β-sheets taking place (~ +6%). The unfolding temperature of $CbA5H_{WT}$ is at ~60 °C (using eq. 1). As a consequence, a drastic reduction in the activity of the enzyme is observed, as shown in Fig. 2. Similar results were obtained for CpI_{WT} (see Figs. SI 1 and Table 1). Furthermore, the van't Hoff enthalpy change of the unfolding process, ΔH_{vH}, could be obtained from the Boltzmann fits. The van't Hoff enthalpy change of CpI_{WT} amounts ~130 kJ mol^{-1} and is only half as large as for the $CbA5H_{WT}$, pointing to a decreased cooperativity of the transition. These values must be handled with caution due to the irreversibility of the heat-induced protein unfolding and subsequent aggregation process, i.e., they reflect no true thermodynamic data and serve only for the comparison.

Figs. 3C-D highlight the pressure dependence on the amide I′ band and the fraction of secondary structures of $CbA5H_{WT}$ as a function of pressure at ambient temperature. The amide I′ band of the hydrogenase is shifting slightly towards lower wavenumbers upon compression, which is due to the pressure-induced compression of the chemical bonds, equivalent to changes of the force constant of the C═O stretching vibration. The fraction of secondary structures changes by a few percent only (± 4%) even up to pressures as high as 10 kbar (Fig. 3D), revealing high pressure stability of the protein structure.

Table 1
Spectroscopically determined unfolding temperatures, T_u, and accompanying van't Hoff enthalpy changes, ΔH_{vH}, of the investigated hydrogenases at ambient pressure.

Hydrogenase	ΔH_{vH} / kJ mol^{-1}	T_u / °C
$CbA5H_{WT}$	228.1 ± 25.4	60.2 ± 3.7
CpI_{WT}	132.8 ± 20	54.3 ± 2.3

3.3. *Pressure dependent enzyme activity followed by oxidation of methyl viologen*

HPSF-measurements were used to investigate pressure effects on the H_2-production activity of $CbA5H_{WT}$ and CpI_{WT} by indirectly tracking the oxidation of methyl viologen at 604 nm. The spectrum of the substrate solution was monitored over a period of time (0–15 s) to track the initial velocity of the enzyme reaction. In order to determine the catalytic activity of the enzyme, the linear segment of the time-dependent UV/Vis absorbance at 604 nm was analyzed (Fig. 4A, inset). As can be clearly seen, the catalytic activity of $CbA5H_{WT}$ remained stable even under elevated pressures up to 2000 bar, the pressure limit of the HPSF apparatus. The pressure-independent activity indicates an activation volume of the reaction that is essentially close to zero. The activation volume is the difference in the partial molar volumes of the transition state ($^{\#}$) and the ground state of the enzyme–substrate complex (ES), i.e., $\Delta V^{\#} = V^{\#} - V_{ES}$. In other words, the structure of the transition state is

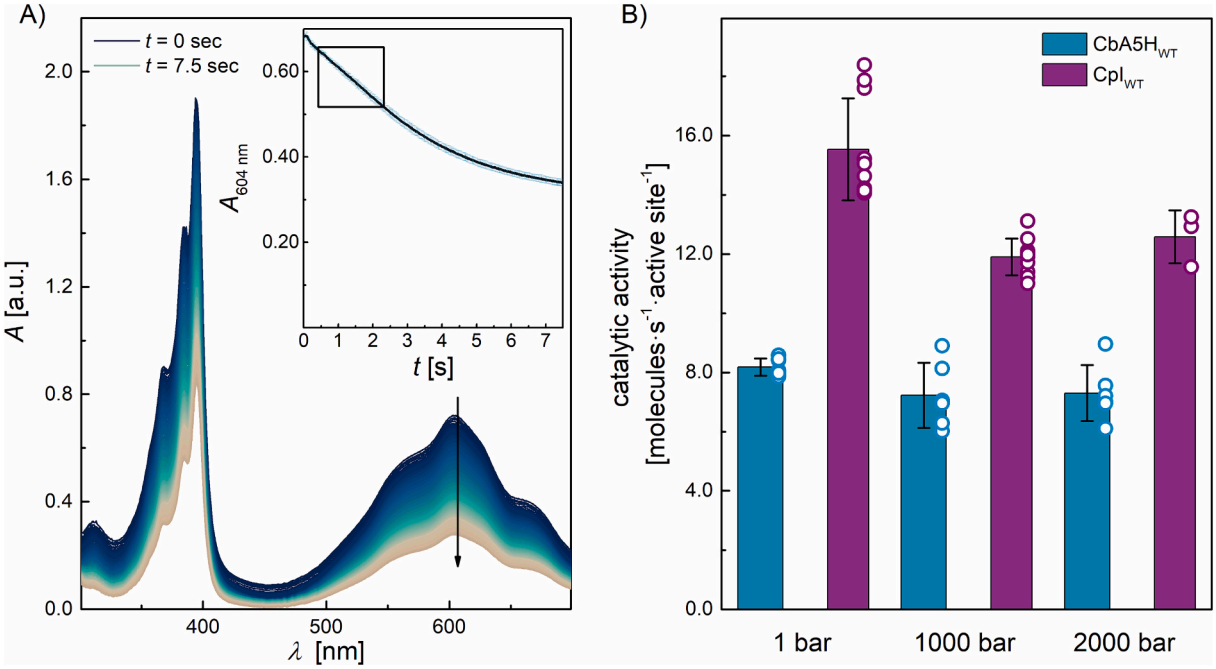

Fig. 4. A) Time dependent absorption spectra of the substrate oxidized by $CbA5H_{WT}$. A wavelength of 604 nm was chosen to follow the time course of the reaction. Inset: Time dependent UV/Vis absorbance at 604 nm of methyl viologen oxidized by $CbA5H_{WT}$ at 1 bar, 25 °C. B) Pressure dependence of the catalytic activity of both hydrogenases at a constant methyl viologen concentration of 80 μM.

similarly compressible as the ES complex in this case. A similar catalytic activity was observed for $CbA5H_{WT}$. In contrast, CpI_{WT} exhibits an about 25% increased catalytic activity compared to $CbA5H_{WT}$. The increased activity of CpI_{WT} also persists up to 2000 bar, mirroring the behavior observed for the other hydrogenase (Fig. 4B). The activity appears to decrease slightly with pressure in this case, only. It can be concluded that there were no significant changes in either the activity or the stability of the secondary structure of these hydrogenases in the whole pressure range covered.

4. Conclusions

The deepest oceans on Earth are populated by organisms that are constantly exposed to high hydrostatic pressure, which reaches values of up to about 1000 bar in the deepest ocean trenches, such as the Mariana trench in the western Pacific Ocean, and in regions below the seafloor [38–41]. Life itself may have been created under pressure, such as in hydrothermal vent environments in the deep sea. Hence, knowledge of HHP effects on biological systems is fundamental to our understanding of life exposed to such harsh conditions, and of the pressure limit of life in general [41]. Of note, microbial communities driven by H_2 have been found in deep-sea settings where other sources of energy, for example from photosynthesis, are not available. Here, we determined the stability and activity of different [FeFe]-hydrogenases from mesophilic bacteria, the $CbA5H_{WT}$ from *Clostridium beijerinckii* and CpI from *C. pasteurianum*, CpI_{WT}, at high temperature and pressure conditions employing FTIR spectroscopy and the high-pressure stopped-flow methodology in concert with fast UV/Vis detection. The two enzymes differ regarding protein structure, stability in the presence of O_2, and in their oligomerization state. While $CbA5H_{WT}$ is a dimer [16], the CpI_{WT} variant acts as monomer. Our data show high temperature stability and a drastically increasing activity up to the unfolding temperatures of the enzymes, which lie at 54–60 °C. Remarkably, both enzymes show a very high structural pressure stability, revealing a high packing density and the absence of a large fraction of internal voids [26,42]. Of note, most proteins unfold at pressures between 2 and 8 kbar, oligomeric ones often also at lower pressures [25,26]. The high pressure stability of the two hydrogenases allows high enzymatic activity up to the 2 kbar range, which largely exceeds the pressure limit encountered by organisms in the deep sea and sub-seafloor on Earth. In future studies, the exploration of hydrogenases from extremophilic microbes that thrive under extremes of temperature and pressure could help answer further questions, such as how protein molecules adapt to function well under such harsh conditions, while their counterparts in mesophiles fail. Furthermore, the understanding of these adaptations could be used in biotechnology to modify enzymes through bioengineering so that they function optimally under specific process conditions [26,41,43].

Credit authorship contribution statement

Kristina Edenharter: Data curation, Formal analysis, Investigation, Methodology, Writing – original draft. **Michel W. Jaworek:** Data curation, Formal analysis, Investigation, Methodology, Writing – original draft. **Vera Engelbrecht:** Data curation, Investigation, Methodology. **Roland Winter:** Conceptualization, Funding acquisition, Supervision, Writing – original draft, Writing – review & editing. **Thomas Happe:** Conceptualization, Funding acquisition, Project administration, Supervision, Writing – review & editing.

Declaration of competing interest

The authors declare that they have no known competing financial interests or personal relationships that could have appeared to influence the work reported in this paper.

Acknowledgements

The authors acknowledge funding from the Deutsche Forschungsgemeinschaft (DFG, German Research Foundation) under Germany's Excellence Strategy – EXC 2033 – project number 390677874-RESOLV. T.H. thanks the Volkswagen Stiftung (Az 98621) and the DFG for funding (HA 2555/10-1).

Appendix A. Supplementary data

Supplementary data to this article can be found online at https://doi.org/10.1016/j.bpc.2024.107217.

References

[1] F.A. Armstrong, J. Hirst, Reversibility and efficiency in electrocatalytic energy conversion and lessons from enzymes, Proc. Natl. Acad. Sci. USA 108 (2011) 14049–14054.
[2] C. Madden, M.D. Vaughn, I. Díez-Pérez, K.A. Brown, P.W. King, D. Gust, A. L. Moore, T.A. Moore, Catalytic turnover of [FeFe]-hydrogenase based on single-molecule imaging, J. Am. Chem. Soc. 134 (2012) 1577–1582.
[3] W. Lubitz, H. Ogata, O. Rüdiger, E. Reijerse, Hydrogenases, Chem. Rev. 114 (2014) 4081–4148.
[4] A.S. Pandey, T.V. Harris, L.J. Giles, J.W. Peters, R.K. Szilagyi, Dithiomethylether as a ligand in the hydrogenase h-cluster, J. Am. Chem. Soc. 130 (2008) 4533–4540.
[5] J. Esselborn, C. Lambertz, A. Adamska-Venkates, T. Simmons, G. Berggren, J. Noth, J. Siebel, A. Hemschemeier, V. Artero, E. Reijerse, M. Fontecave, W. Lubitz, T. Happe, Spontaneous activation of [FeFe]-hydrogenases by an inorganic [2Fe] active site mimic, Nat. Chem. Biol. 9 (2013) 607–609.
[6] G. Berggren, A. Adamska, C. Lambertz, T.R. Simmons, J. Esselborn, M. Atta, S. Gambarelli, J.M. Mouesca, E. Reijerse, W. Lubitz, T. Happe, V. Artero, M. Fontecave, Biomimetic assembly and activation of [FeFe]-hydrogenases, Nature 499 (2013) 66–69.
[7] A. Silakov, B. Wenk, E. Reijerse, W. Lubitz, ^{14}NHYSCORE investigation of the h-cluster of [FeFe] hydrogenase: evidence for a nitrogen in the dithiol bridge, Phys. Chem. Chem. Phys. 11 (2009) 6592–6599.
[8] B.J. Lemon, J.W. Peters, Binding of exogenously added carbon monoxide at the active site of the iron-only hydrogenase (CpI) from *clostridium pasteurianum*, Biochemistry 38 (1999) 12969–12973.
[9] J.W. Peters, W.N. Lanzilotta, B.J. Lemon, L.C. Seefeldt, X-ray crystal structure of the Fe-only hydrogenase (CpI) from *Clostridium pasteurianum* to 1.8 angstrom resolution, Science 282 (1998) 1853–1858.
[10] Y. Nicolet, B.J. Lemon, J.C. Fontecilla-Camps, J.W. Peters, A novel FeS cluster in Fe-only hydrogenases, Trends Biochem. Sci. 25 (2000) 138–143.
[11] Y. Nicolet, C. Piras, P. Legrand, C.E. Hatchikian, J.C. Fontecilla-Camps, Desulfovibrio desulfuricans iron hydrogenase: the structure shows unusual coordination to an active site Fe binuclear center, Structure 7 (1999) 13–23.
[12] J. Meyer, [FeFe] hydrogenases and their evolution: a genomic perspective, Cell. Mol. Life Sci. 64 (2007) 1063–1084.
[13] C.E. Lubner, J.H. Artz, D.W. Mulder, A. Oza, R.J. Ward, S.G. Williams, A.K. Jones, J.W. Peters, I.I. Smalyukh, V.S. Bharadwaj, P.W. King, A site-differentiated [4Fe-4S] cluster controls electron transfer reactivity of *clostridium acetobutylicum* [FeFe]-hydrogenase I, Chem. Sci. 13 (2022) 4581–4588.
[14] P.S. Corrigan, J.L. Tirsch, A. Silakov, Investigation of the unusual ability of the [FeFe] hydrogenase from *Clostridium beijerinckii* to access an O_2-protected state, J. Am. Chem. Soc. 142 (2020) 12409–12419.
[15] S. Morra, M. Arizzi, F. Valetti, G. Gilardi, Oxygen stability in the new [FeFe]-hydrogenase from *Clostridium beijerinckii* SM10 (CbA5H), Biochemistry 55 (2016) 5897–5900.
[16] M. Winkler, J. Duan, A. Rutz, C. Felbek, L. Scholtysek, O. Lampret, J. Jaenecke, U.-P. Apfel, G. Gilardi, F. Valetti, V. Fourmond, E. Hofmann, C. Léger, T. Happe, A safety cap protects hydrogenase from oxygen attack, Nat. Commun. 12 (2021) 756.
[17] M. Winkler, J. Esselborn, T. Happe, Molecular basis of [FeFe]-hydrogenase function: an insight into the complex interplay between protein and catalytic cofactor, Biochim. Biophys. Acta Bioenerg. 1827 (2013) 974–985.
[18] J.W. Peters, G.J. Schut, E.S. Boyd, D.W. Mulder, E.M. Shepard, J.B. Broderick, P. W. King, M.W.W. Adams, [FeFe]- and [NiFe]-hydrogenase diversity, mechanism, and maturation, Biochim. Biophys. Acta, Mol. Cell Res. 1853 (2015) 1350–1369.
[19] M.W. Jaworek, N.F. Gajardo-Parra, G. Sadowski, R. Winter, C. Held, Boosting the kinetic efficiency of formate dehydrogenase by combining the effects of temperature, high pressure and co-solvent mixtures, Colloids Surf. B: Biointerfaces 208 (2021) 112127.
[20] M.W. Jaworek, R. Winter, Exploring enzymatic activity in multiparameter space: cosolvents, macromolecular crowders and pressure, ChemSystemsChem 3 (2021) e2000029.
[21] C. Schuabb, N. Kumar, S. Pataraia, D. Marx, R. Winter, Pressure modulates the self-cleavage step of the hairpin ribozyme, Nat. Commun. 8 (2017) 14661.
[22] T.Q. Luong, N. Erwin, M. Neumann, A. Schmidt, C. Loos, V. Schmidt, M. Fändrich, R. Winter, Hydrostatic pressure increases the catalytic activity of amyloid fibril enzymes, Angew. Chem. Int. Ed. 55 (2016) 12412–12416.
[23] E. Decaneto, S. Suladze, C. Rosin, M. Havenith, W. Lubitz, R. Winter, Pressure and temperature effects on the activity and structure of the catalytic domain of human MT1-MMP, Biophys. J. 109 (2015) 2371–2381.
[24] T.Q. Luong, R. Winter, Combined pressure and cosolvent effects on enzyme activity - a high-pressure stopped-flow kinetic study on α-chymotrypsin, Phys. Chem. Chem. Phys. 17 (2015) 23273–23278.
[25] K. Akasaka, H. Matsuki, High Pressure Bioscience, Springer, Netherlands, Dordrecht, 2015.
[26] R. Winter, Interrogating the structural dynamics and energetics of biomolecular systems with pressure modulation, Annu. Rev. Biophys. 48 (2019) 441–463.
[27] V.V. Mozhaev, K. Heremans, J. Frank, P. Masson, C. Balny, High pressure effects on protein structure and function, Proteins 24 (1996) 81–91.
[28] L. Ostermeier, M. Ascani, N. Gajardo-Parra, G. Sadowski, C. Held, R. Winter, Leveraging liquid-liquid phase separation and volume modulation to regulate the enzymatic activity of formate dehydrogenase, Biophys. Chem. 304 (2024) 107128.
[29] M.E. Gerringer, P.H. Yancey, O.V. Tikhonova, N.E. Vavilov, V.G. Zgoda, D. R. Davydov, Pressure tolerance of deep-sea enzymes can be evolved through increasing volume changes in protein transitions: a study with lactate dehydrogenases from abyssal and hadal fishes, FEBS J. 287 (2020) 5394–5410.
[30] M. Panda, P.M. Horowitz, Activation parameters for the spontaneous and pressure-induced phases of the dissociation of single-ring GroEL (SR1) chaperonin, Protein J. 23 (2004) 85–94.
[31] J.M. Kuchenreuther, C.S. Grady-Smith, A.S. Bingham, S.J. George, S.P. Cramer, J. R. Swartz, High-yield expression of heterologous [FeFe] hydrogenases in Escherichia coli, PLoS One 5 (2010) e15491.
[32] U.K. Laemmli, Cleavage of structural proteins during the assembly of the head of bacteriophage T4, Nature 227 (1970) 680–685.
[33] P.T.T. Wong, D.J. Moffat, A new internal pressure calibrant for high-pressure infrared spectroscopy of aqueous systems, Appl. Spectrosc. 43 (1989) 1279–1281.
[34] A. Barth, Infrared spectroscopy of proteins, Biochim. Biophys. Acta Bioenerg. 1767 (2007) 1073–1101.
[35] J.L. Arrondo, A. Muga, J. Castresana, F.M. Goñi, Quantitative studies of the structure of proteins in solution by Fourier-transform infrared spectroscopy, Prog. Biophys. Mol. Biol. 59 (1993) 23–56.
[36] P. Bugnon, G. Laurenczy, Y. Ducommun, P.Y. Sauvageat, A.E. Merbach, R. Ith, R. Tschanz, M. Doludda, R. Bergbauer, E. Grell, High-pressure stopped-flow spectrometer for kinetic studies of fast reactions by absorbance and fluorescence detection, Anal. Chem. 68 (1996) 3045–3049.
[37] S.G. Mayhew, The redox potential of dithionite and SO_2^- from equilibrium reactions with flavodoxins, methyl viologen and hydrogen plus hydrogenase, Eur. J. Biochem. 85 (1978) 535–547.
[38] P.H. Yancey, M.E. Gerringer, J.C. Drazen, A.A. Rowden, A. Jamieson, Marine fish may be biochemically constrained from inhabiting the deepest ocean depths, Proc. Natl. Acad. Sci. USA 111 (2014) 4461–4465.
[39] I. Daniel, P. Oger, R. Winter, Origins of life and biochemistry under high-pressure conditions, Chem. Soc. Rev. 35 (2006) 858–875.
[40] J.L. Silva, A.C. Oliveira, T.C.R.G. Vieira, G.A.P. de Oliveira, M.C. Suarez, D. Foguel, High-pressure chemical biology and biotechnology, Chem. Rev. 114 (2014) 7239–7267.
[41] J.-M. Knop, S. Mukherjee, M.W. Jaworek, S. Kriegler, M. Manisegaran, Z. Fetahaj, L. Ostermeier, R. Oliva, S. Gault, C.S. Cockell, R. Winter, Life in multi-extreme environments: brines, osmotic and hydrostatic pressure - a physicochemical view, Chem. Rev. 123 (2023) 73–104.
[42] J. Roche, J.A. Caro, D.R. Norberto, P. Barthe, C. Roumestand, J.L. Schlessman, A. E. Garcia, B.E. García-Moreno, C.A. Royer, Cavities determine the pressure unfolding of proteins, Proc. Natl. Acad. Sci. USA 109 (2012) 6945–6950.
[43] M.J. Eisenmenger, J.I. Reyes-De-Corcuera, High pressure enhancement of enzymes: a review, Enzym. Microb. Technol. 45 (2009) 331–347.